Microtexture and Chitin/Calcite Orientation Relationship in the Mineralized Exoskeleton of the American Lobster**

By *Ali Al-Sawalmih, Chenghao Li, Stefan Siegel, Helge Fabritius, Sangbong Yi, Dierk Raabe, Peter Fratzl,* and *Oskar Paris**

The exoskeleton of the American lobster *Homarus americanus* is a hierarchical nanocomposite consisting of chitin–protein fibers, reinforced with amorphous calcium carbonate (ACC) and a small amount of crystalline calcite. Crystallographic pole-figure analysis reveals two texture components of the crystalline α-chitin in the exoskeleton. One component represents the well-known twisted plywood structure of chitin–protein fibers within the cuticle plane, and the second component represents fibers oriented roughly perpendicular to the cuticle surface. These perpendicular fibers interpenetrate the open canals of the planar honeycomblike structure originating from the well-developed pore-canal system present in this material. The calcite crystallites reveal fiber texture with the crystallographic *c*-axis oriented perpendicular to the cuticle surface, suggesting an orientation relationship between calcite and the organic chitin–protein fibers. Local orientation analysis using X-ray microdiffraction reveals that the crystalline calcium carbonate fraction is associated with the chitin–protein fibers oriented perpendicular to the surface. Calcite is exclusively found in the exocuticle and is mostly restricted to a thin layer in the outermost region, while the major part of the exocuticle and the whole endocuticle contain ACC exclusively. It is therefore speculated that the most likely function of calcite in the exoskeleton of the American lobster is related to impact- and wear-resistance.

1. Introduction

Crustaceans, which include a multitude of organisms such as lobsters, crabs, or shrimps incorporate inorganic minerals into the organic matrix of their exoskeleton, which is formed by the cuticle.[1] This process is referred to as biomineralization, since it is biologically controlled by the organism.[2] The biominerals formed in crustaceans are typically amorphous calcium carbonate (ACC) with some small amounts of amorphous calcium phosphate (ACP), as well as varying amounts of crystalline calcite.[3,4] ACC is a polymorph of low stability which — in an uncontrolled environment — tends to transform into more stable crystalline phases.[5] It is well known that the amorphous phases incorporated in the cuticle can be stabilized by specific proteins or metal ions (e.g., Mg).[6–12] The formation of ACC in the crustacean cuticle and its possible transformation into a stable crystalline polymorph has not been investigated as intensively as, for instance, in mollusc shells.[13,14] The detailed functional role of calcium carbonate biominerals associated with the exoskeleton of crustaceans is still a matter of debate, although two main functions — calcium storage and mechanical strengthening[6,12] — seem to be generally accepted. Several structural studies on crustacean exoskeleton mineralization have been performed, in particular for crabs.[1,15–19] Nonetheless, many details about the local nanostructure, as well as the morphological and crystallographic texture of the minerals within the hierarchically organized organic matrix in the crustacean exoskeleton, are still largely unknown.

Crustacean cuticle is composed chiefly of organic fibers closely associated with calcium carbonate,[1,10,11,20] showing a distinct structural hierarchy from the nanometer to the millimeter scale. The most prominent structural units are the chitin/protein fibers composed of bundles of nanofibrils which — according to the model of Blackwell and Weih[21,22] — consist of about 10–20 antiparallel chains of α-chitin wrapped by proteins. These chitin–protein fibers have diameters of the order of 50–300 nm and form planar layers in the cuticle.[23] These are then stacked in a twisted plywood pattern, which is characteristic of the cuticle of most arthropods.[21,24–26] The lobster possesses an extremely well developed pore-canal system oriented perpendicular to the cuticle surface. These pore canals have a diameter of about 1 μm and penetrate the twisted plywood structure more or less perpendicularly, leading to a 3D structure that resembles a honeycomb.[23] A second class of α-chitin–protein fibers was found to interpenetrate the

[*] Dr. O. Paris, Dr. A. Al-Sawalmih, Dr. C. Li, Dr. S. Siegel, Prof. P. Fratzl
Department of Biomaterials, Max-Planck Institute for Colloids & Interfaces
Research Campus Golm, 14424 Potsdam (Germany)
E-mail: Oskar.Paris@mpikg.mpg.de
Dr. H. Fabritius, Prof. D. Raabe
Max-Planck-Institut für Eisenforschung
Max-Planck-Str. 1, 40237 Düsseldorf (Germany)
Dr. S. B. Yi
Institute of Materials Research, GKSS-Forschungszentrum
Max-Planck-Str. 1, 21502 Geesthacht (Germany)

FULL PAPER

network along these canals perpendicular to the cuticle surface.[27]

The mineral component in lobster cuticle consists mainly of ACC with small amounts of ACP and calcite.[3,10] Similar to many other arthropods, the ratio of crystalline to amorphous calcium carbonate can vary considerably within the given species.[3,4] We refer to the crystalline mineral as calcite, even though it typically incorporates variable amounts of Mg ions, similar to the ACC.[10,28,29] While for fast release of calcium ions the amorphous polymorph is clearly advantageous, the benefits of amorphous versus crystalline calcium carbonate for the mechanical properties of the cuticle are not so obvious and have previously been discussed in more detail by Addadi et al.[6] It might also be possible that some of the metastable ACC crystallizes due to some unfavorable external influences at specific sites, where the subtle biological control of the biomineralization by specific proteins is missing.[7,12] Thus, identifying the crystallization sites of calcite in lobster cuticle and their association with the organic matrix is of essential importance to yield a better understanding of both the biomineralization process and the functional role of the crystalline calcium carbonate.

In order to answer these questions, we have investigated the local organization of calcite and its interaction with the hierarchically organized organic matrix using X-ray texture analysis, a method well established in materials science.[30] Moreover, we employ synchrotron-radiation-based microbeam X-ray diffraction to obtain position-resolved information on the type and local texture of the biominerals in the exoskeleton of the American lobster.

2. Results and Discussion

A typical 2D diffraction pattern from the lobster cuticle with the X-ray beam roughly parallel to the cuticle surface is shown in Figure 1a, and the corresponding 1D diffraction profile obtained by azimuthally averaging the 2D pattern is displayed in Figure 1b. Here, the modulus of the scattering vector q is defined by $q = 4\pi\sin\theta/\lambda$, with λ being the X-ray wavelength and 2θ the scattering angle. Reflections from both chitin (orthorhombic, space group $P2_12_12_1$, $a = 4.74$ Å, $b = 18.86$ Å, $c = 10.32$ Å)[31] and calcite (rhombohedral, space group $R3c$, $a = 4.989$ Å, $c = 17.062$ Å)[32] are clearly discernable, and the strongest reflections are indicated by the corresponding Miller indices. The calcite reflections are rather weak owing to the fact that the major part of the mineral in lobster is present in the form of ACC, which is clearly demonstrated by the broad, diffuse scattering intensity in the range $q \approx 18$–26 nm^{-1}.

Figure 2 displays pole figures from selected calcite and chitin reflections. The pole figures clearly suggest a crystallographic orientation relationship between calcite (left column) and chitin (right column). The {00.6} and {11.0} pole figures from calcite indicate a simple fiber texture in the crystalline mineral phase with the c-axis pointing into the direction N perpendi-


(a)

(b)
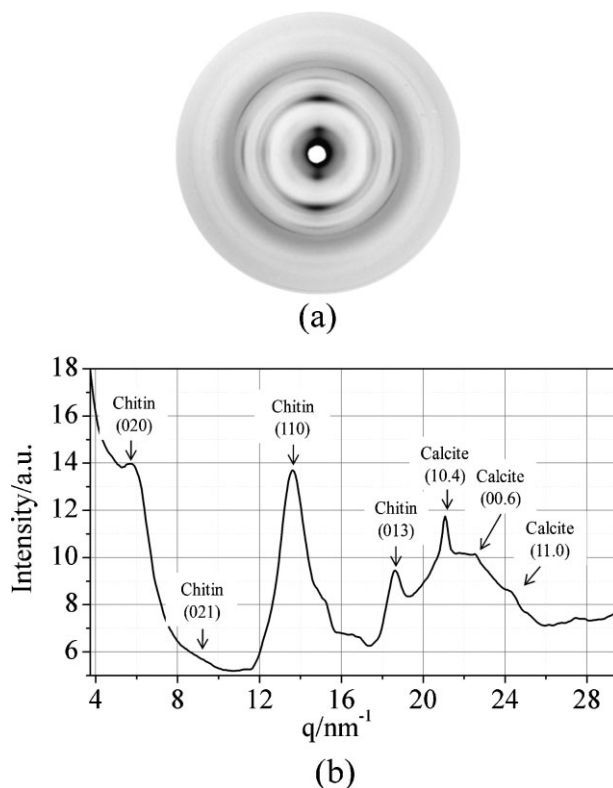
Figure 1. a) 2D diffraction pattern obtained from lobster cuticle. The X-ray beam direction is approximately parallel to the cuticle surface which is horizontal in the figure. b) Diffraction profiles obtained by azimuthally averaging the 2D pattern shown in a). The most prominent reflections of chitin and calcite are indexed.

cular to the cuticle surface (see the definition of the coordinate system in Fig. 2). The texture of chitin is more complicated and must be related carefully to the actual microstructure of the organic matrix. In the following we discuss the pole figures of Figure 2 with respect to two important aspects: the relation between the chitin texture and the hierarchical microstructure of the fibrous cuticle tissue (Sec. 2.1), and the orientation relationship between calcite and chitin and its microstructural implications (Sec. 2.2). We then present scanning (in-situ) X-ray microbeam diffraction results on the spatial distribution of calcite and ACC in the cuticle (Sec. 2.3). Based on the resulting comprehensive structural and microtextural picture, we finally discuss the possible functional role of crystalline calcite and ACC in the lobster cuticle (Sec. 2.4).

2.1. Chitin Texture

2.1.1. Chitin c-Axis (Fiber Axis)

The chitin c-axis is parallel to the molecular chain axis and thus to the morphological fiber axis. Since the corresponding chitin 002 reflection occurs very close to the strong and broad 110 reflection (Fig. 1b), they overlap and (002) is unfortunately too weak to be used for a reliable pole-figure construction.
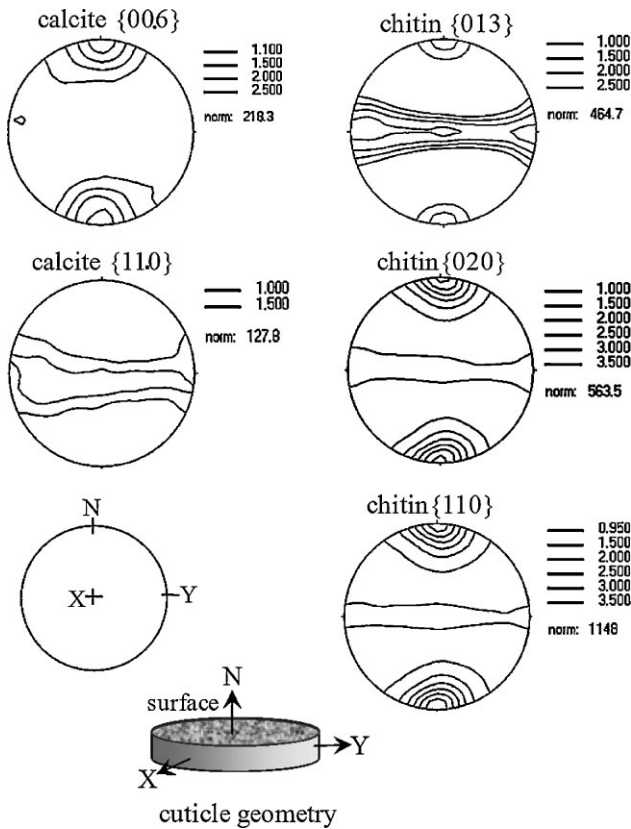
Figure 2. Selected pole figures from lobster arranged to underline the orientation relationship between calcite (left) and α-chitin (right) with respect to the cuticle geometry. The sample reference system is included, with N representing the normal (or surface) direction; X and Y represent the two equivalent orthogonal directions within the cuticle plane.

However, the ⟨013⟩ and ⟨01̄3⟩ directions in the chitin unit cell deviate from the c-direction by only about ±10°. Owing to some broadening (Fig. 1a), the 013 and 01̄3 reflections overlap azimuthally and merge into one single broad maximum centered on the polymer-chain axis direction. Consequently, the {013} pole figure can be used to describe the morphological texture of the chitin fibers, being equivalent to the direction of the c-axis of chitin. The {013} chitin pole figure in Figure 2a shows a strong texture component within the cuticle plane (X–Y plane) and a somewhat weaker component in normal direction N to the cuticle surface. The in-plane component can be attributed to the twisted plywood structure of chitin fibers within the cuticle plane, and the second component can be attributed to fibers oriented perpendicular to the cuticle surface. This texture pattern has already been reported previously, and electron microscopy revealed that the perpendicular fibers are located within and along the cavities of the pore canals that create the honeycomblike structure of the chitin–protein fiber layers (see also Fig. 5).[23,27,33]

2.1.2. Chitin b-Axis

The {020} pole figure (Fig. 2) also shows two components that can be related to the in-plane and out-of-plane

components mentioned above. The out-of plane component is characterized by a homogeneous intensity distribution of the 020 reflection in the X–Y plane implying fiber symmetry around the morphological fiber axis. The second (in-plane) component appears to be more complex. The corresponding {020} pole figure suggests a strong preferred orientation of the b-axis towards the cuticle surface, which seems to indicate that the individual fibers are single crystalline entities with the b-axis being perpendicular to the cuticle surface. Such an interpretation would however imply that the in-plane chitin fibers are different from the out-of-plane fibers. These are obviously rotationally symmetric around the chitin c-axis, which corresponds to the morphological fiber axis. Moreover, the {110} pole figure (Fig. 2) is identical to the {020} pole figure which is in contradiction with a simple fiber texture of the in-plane component.

We can resolve this puzzling texture phenomenon by assuming that each individual chitin fiber exhibits fiber symmetry around the morphological fiber axis, and noting the fact that a second (perpendicular) fiber axis is generated by the plywood structure. Figure 3 presents a sketch which qualitatively explains the chitin texture of the in-plane fiber component. The "intensity" distributions in reciprocal space for single in-plane and out-of-plane fibers are sketched in Figure 3a and b, respectively. Only one equatorial reflection hk0 that smears into a ring due to the fiber symmetry, and one meridional reflection 00l are shown for better clarity. The twisted plywood structure of the in-plane fiber component implies that the hk0 rings of Figure 3a are randomly rotated around the cuticle normal N which is perpendicular to the fiber axis c*. This means that the intensity of the hk0 reflections smears out homogeneously onto a sphere, with the only exception of the common pole N, where all contributions add to give a much higher intensity. This is sketched in Figure 3c, by assuming a certain broadening of the rings due to slight deviations from a perfect in-plane orientation. The 00l reflections on the other hand smear into rings (Fig. 3c). We call this type of texture a pseudofiber texture, since the two perpendicular fiber axes create a fiber texture pattern with the crystallographic fiber axis perpendicular to the morphological fiber axis. Together with the simple fiber pattern of the out-of-plane component (Fig. 3b), the measured diffraction pattern (Fig. 3d), and in particular also the chitin pole figures in Figure 2 can be fully described by this picture.

2.2. Orientation Relation between Calcite and Chitin

The next point to discuss is the orientation relationship between calcite and chitin crystallites. Calcite exhibits a simple fiber texture with the c-axis perpendicular to the cuticle surface (Fig. 2). According to the above discussion of the chitin texture, we can deduce two possibilities for the crystallographic orientation relationship between the calcite c-axis and the chitin c-axis, and the corresponding association with one of the two chitin fiber components: i) the calcite c-axis is *parallel* to the chitin c-axis with the calcite being associated with the
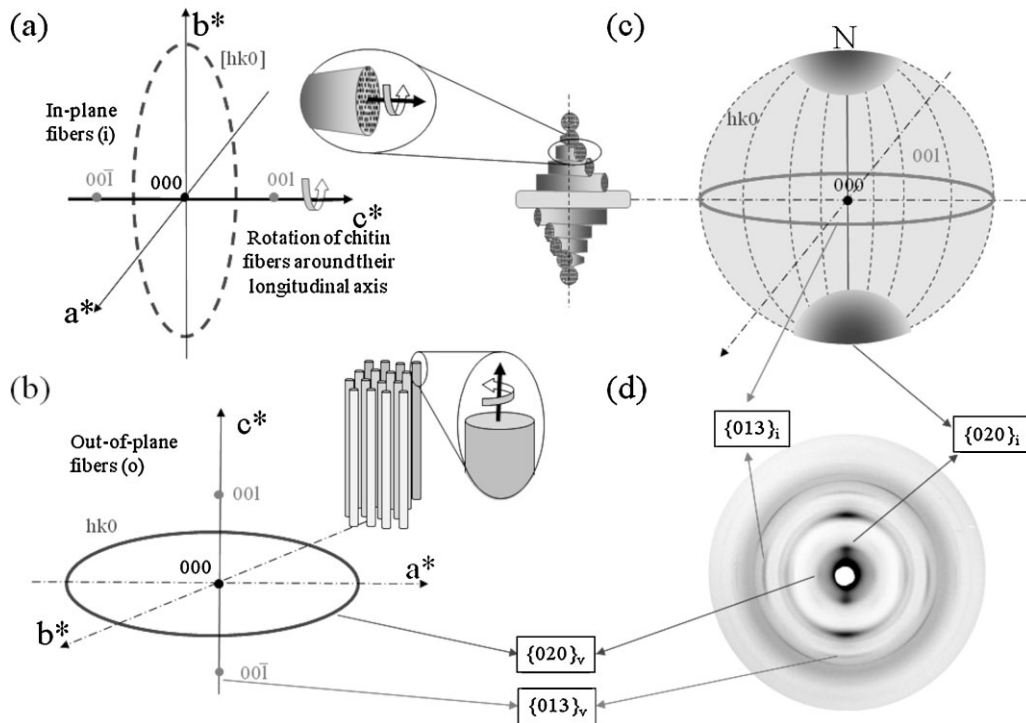
Figure 3. Sketch to illustrate the relation between measured texture and the hierarchical microstructure of the chitin fibers. Each single chitin fiber is supposed to exhibit crystallographic fiber symmetry around the morphological fiber axis, which corresponds to the crystallographic c-axis of chitin. This leads to characteristic fiber patterns in reciprocal space (a, b), i.e., the equatorial reflections are smeared on rings around the fiber axis c^*. Since the in-plane fibers are arranged in a rotated plywood structure within the cuticle plane, the intensity of the equatorial reflections of this component is homogeneously smeared on a sphere (c), with the only exception of the normal direction N, where all contributions add to yield a much higher intensity. At the same time, the original meridional 001 reflections are smeared on a ring perpendicular to N, which leads to a pseudo-fiber pattern. The measured diffraction pattern (d) is composed of this pseudo-fiber pattern and the true fiber pattern from the vertical fiber component.

out-of-plane fibers or ii) the calcite c-axis is *perpendicular* to the chitin c-axis with the calcite being associated with the in-plane fibers. Analyzing the pole figures (Fig. 2) in more detail, one finds that the two chitin fiber components are not exactly perpendicular to each other. The deviation is, however too small to relate the calcite unambiguously to one of the two components, since a large sample volume (around $1 \, mm^3$) was illuminated by the beam.

To prove the association of the calcite with one of the occurring chitin fiber orientations, we investigated the local orientation by scanning microbeam X-ray diffraction using a $10 \, \mu m$ X-ray beam. Several parallel line scans with a step size of $10 \, \mu m$ were performed across the epicuticle, exocuticle, and endocuticle with the X-ray beam perpendicular to the cuticle normal N. Figure 4 shows a representative 2D diffraction pattern obtained from a region in the exocuticle close to the exocuticle/endocuticle interface. A clear tilt of the out-of-plane fibers with respect to the cuticle normal N (by both, the 020 and the 013 reflections) is observed. Also, the c-axis of the in-plane fiber component is not exactly perpendicular to the cuticle normal N, but slightly tilted. This means that the two chitin fiber components are locally (within the position resolution of $10 \, \mu m$) not exactly perpendicular with respect to each other due to the wavy structure of the plywood lamellae (Fig. 5a).

Interestingly, the azimuthal tilt of the calcite 00.6 reflection corresponds exactly to the one of the chitin 013 reflection of the out-of-plane chitin fiber component suggesting the association of the calcite with the out-of-plane chitin fibers. Figure 4b visualizes this fact more clearly by showing isolated azimuthal profiles of the three most important reflections. The $(00.6)_{calcite}$ and the $(013)_{chitin}$ reflection from the out-of-plane component are clearly collinear, while $(020)_{chitin}$ from the in-plane component is shifted by about $15°$. Even though we could not perform a full texture analysis with the microbeam setup, the fact that the c-axis of calcite is exactly parallel the c-axis of chitin strongly indicates that the crystalline calcite in lobster cuticle is associated with the out-of-plane fiber component.

2.3. Mineral Localization

Besides the association of the calcite c-axis with the out-of-plane chitin fiber direction, the microbeam X-ray diffraction experiment gave additional information about the localization of the two major mineral phases calcite and ACC. Diffraction patterns were measured in several line scans across the cuticle cross-section covering epicuticle, exocuticle and endocuticle (see Fig. 5a). Calcite was consistently found in the distal layers
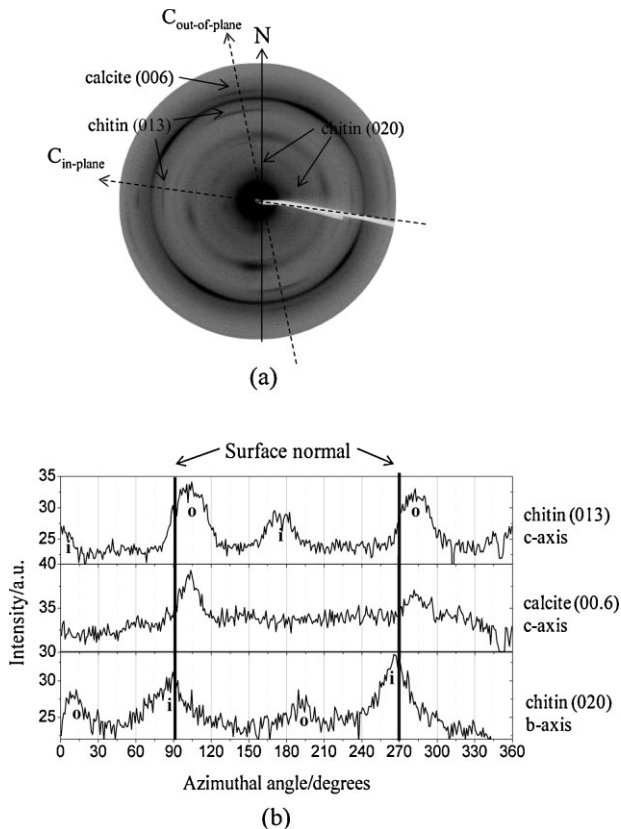
Figure 4. a) Microbeam diffraction pattern from the calcified lobster exocuticle recorded with the X-ray beam parallel to the cuticle surface. The *c*-axis of the out-of-plane fiber component is tilted with respect to the cuticle normal N. The azimuthal coincidence of the calcite 00.6 reflection and the chitin $013/0\bar{1}3$ pair indicates that the calcite *c*-axis and the chitin *c*-axis of the vertical fiber component are collinear. b) Azimuthal profile of selected α-chitin and calcite reflections from the 2D pattern in (a). The notations "o" and "i" represent the components belonging to the out-of-plane fibers and the in-plane fibers, respectively.

of the exocuticle in a region extending about 20–50 μm from the epicuticle/exocuticle interface. Additionally, some calcite appeared to be heterogeneously distributed within a few "clusters" located in the exocuticle with some preference close to the exocuticle/endocuticle interface. Surprisingly, crystalline calcite was not detected in the endocuticle. This was confirmed by repeating the microbeam scanning experiment with a second specimen from a different animal. In order to verify that the whole cuticle is fully mineralized and contains ACC in the non calcified regions, this sample was used for an in situ heating experiment within the X-ray microbeam, by which we could prove the temperature induced transformation of ACC into calcite. Figure 6 shows diffraction profiles for three different temperatures from the same representative region within the endocuticle. There are only slight changes in the diffraction patterns for temperatures up to about 250 °C, indicating that the thermal stability of the chitin crystal structure is similar to that of cellulose.[34] The crystalline chitin decomposed completely at temperatures between 250–300 °C, and only a

broad hump from ACC remained in the diffraction profile at 325 °C. At about 425 °C, the amorphous halo from ACC started to vanish, and calcite reflections appeared. The whole cuticle was fully calcified at 450 °C indicating that ACC has fully transformed into calcite (see Fig. 6). This experiment clearly demonstrated that the major part of the lobster cuticle is mineralized with ACC. The thermally transformed calcite showed perfect powder rings, while the biologically formed calcite layer in the distal exocuticle layer did not change at all with thermal treatment, neither in its texture pattern, nor in its lattice parameter after cooling back to room temperature.

2.4. Calcium Carbonate in the Exoskeleton and its Possible Functional Role

The present study revealed a thin calcite-containing layer in the outermost exocuticle of the American lobster, while the rest of the fully mineralized exoskeleton contains mostly amorphous calcium carbonate (ACC). The calcite in this layer has a unique orientation with the *c*-axis pointing perpendicular to the cuticle surface and being associated with out-of-plane chitin fibers situated in the pore canals. A similar crystallographic arrangement has been found in mollusk shells where the outer layer contains crystalline calcite (prismatic layer) and is parallel to the inner nacreous layer (mother-of pearl) consisting mainly of aragonite. X-ray texture studies indicated that the *c*-axis of the calcite prisms and aragonite tablets are oriented perpendicular to the shell surface, while the *a*- and *b*-axes of the crystals within a stack are co-aligned.[35,36] In the egg shell of chicken, the palisade layer makes up the majority of the calcified portion of the shell. The large crystals of calcite are also oriented with their *c*-axes perpendicular to the surface of the shell.[37,38] Thus, a calcite *c*-axis orientation perpendicular to the outer surface seems to be common also for other mineralized structures in nature.
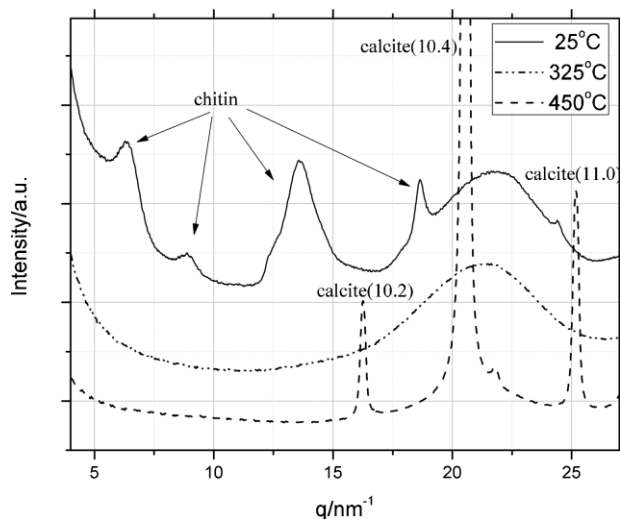
As compared to mollusk shells, much less is known about the biomineralization process and the functional role of calcite and ACC in the exoskeleton of crustaceans. The best investigated crustaceans in terms of biomineralization are crabs. In contrast to lobster cuticle, the crab cuticle is almost fully calcified in the intermolt state, even though the initial mineral deposited seems to be ACC which is subsequently calcified.[18] It was already noted by Bouligand, cited by Neville[1] that the orientation of calcite crystallites in the shore crab (*Carcinus maenas*) does not follow the helicoidal orientation of the organic matrix. Quite some subsequent work on crabs concentrated on mineral localization and on the mineralization process during the molting cycle,[16–19,39–41] however, the picture about calcite orientation in crab cuticle seems not to be fully consistent and complete in the literature. A recent texture study in giant barnacles (*Austromegabalanus psittacus*)[42] revealed a calcite *c*-axis orientation perpendicular to the cuticle surface in the external shell, in agreement to the present work. Interestingly, in the internal shell shield the authors found a calcite texture with the *c*-axis parallel to the shell, suggesting a different role of the calcite in different regions.
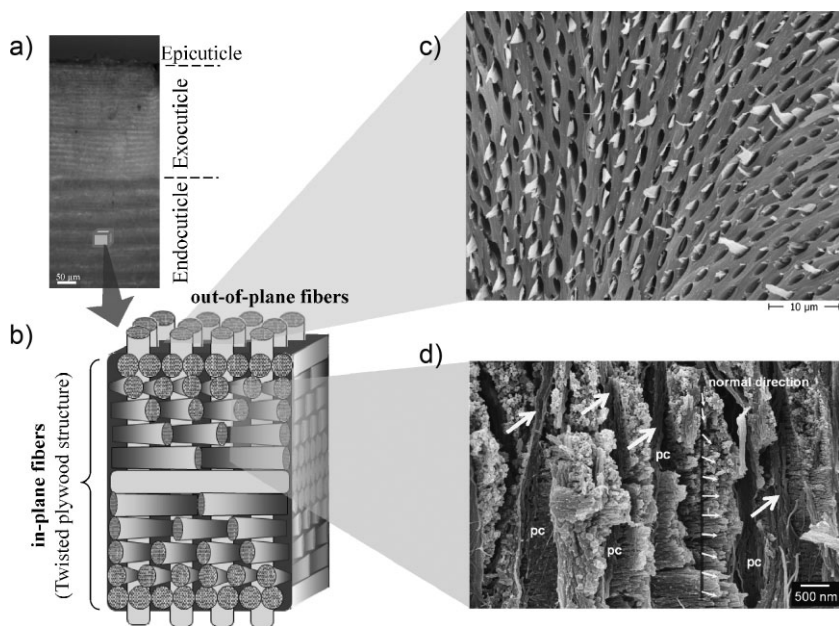
Figure 5. Summary of the major structural features of lobster cuticle at the micrometer level. a) Optical micrograph from a cross section of the cuticle shows the epicuticle and the lamellar structure of the exocuticle and the endocuticle. b) Sketch showing the in-plane fibers forming a rotated plywood structure within the cuticle plane with interpenetrating out-of-plane fibers associated with calcite. c) SEM image of the chitin–protein planes within one in-plane layer, showing pore canal tubes which belong to the ion transport system. d) SEM image of cross-fractured cuticle from the carapace of the lobster showing the plywood structure formed by the rotating in-plane chitin protein fibers (thin arrows) and the out-of-plane chitin protein fibers (thick arrows) arranged along the cavities of the pore canals (pc).

It is well known that the amount of crystalline and amorphous mineral phases can vary considerably amongst different crustaceans.[3,4] The lobster cuticle has particularly low calcite content and a very high ACC content.[6,43] No specific information about the spatial distribution of these two phases in lobster cuticle was available to our knowledge so far. The present work indicates that the spatial location of ACC and calcite and their relation to the organic matrix may be controlled by subtle biological mechanisms. The spatial separation of the calcite and ACC, and the unique orientation of the outer crystalline layer suggest a specific mechanical function in lobster cuticle. Oriented calcite columns along the pore canals will stiffen the material in the direction normal to the cuticle surface which is the impact direction. Hence, this structural feature makes penetration of the cuticle more difficult by stopping the penetrator, while the underlying, more elastic ACC-reinforced part of the cuticle can dissipate the acting impact energy. Moreover, an outermost layer of crystalline calcite is certainly also very advantageous for the wear resistance of the cuticle. Together with the obvious advantages of ACC with respect to solubility, ability to form complex mineral shapes, and isotropy of mechanical properties,[8,18] the lobster cuticle appears to be a highly sophisticated functional material. Finally, it cannot be excluded that the calcite-stiffened vertical fibers might also be involved into a sensory function by transmitting strain- or optical signals from the cuticle surface.

3. Conclusions

The exoskeleton of the American lobster (*Homarus americanus*) is a highly sophisticated, hierarchically structured material consisting of a fibrous network of chitin–protein nanofibrils reinforced with amorphous calcium carbonate as well as with crystalline calcite. The major structural features of the lobster cuticle at the micrometer level are summarized in Figure 5. The in-plane twisted plywood structure is a general feature of many natural fibrous tissues and is well known to be beneficial for the mechanical performance of the crustacean exoskeleton.[44,45] The present work provides for the first time evidence that a second class of chitin–protein fibers — interpenetrating the in-plane plywood structure through a well developed pore canal system — is uniquely associated with well oriented crystalline calcite in a thin surface layer in the distal region of the exocuticle. These chitin–protein fibers presumably

Figure 6. Microbeam X-ray diffraction profiles from the endocuticle of the lobster. There are chitin reflections but no indication of any calcite reflections at room temperature. At 325 °C, the crystalline chitin has fully decomposed and only a broad hump from ACC remains. At 450 °C, the ACC is almost entirely transformed into calcite as can be seen by the corresponding calcite reflection and the diminished amorphous peak. The profiles are shifted with respect to the vertical axis for clarity.

assist the orientated growth of calcite by either acting as a template with specific crystal growth occurring on active sites on the surface[13] or within the organic fibers. Except of this calcified layer, the whole rest of the cuticle is essentially reinforced with highly stabilized amorphous calcium carbonate. The biological control and the factors inhibiting the transformation of the ACC into crystalline calcite in the inner layers of the cuticle in lobster are however not yet clear, and touch one of the most pressing questions in biomineralization. The absence of calcite in the endocuticle, and its abundant occurrence at the outermost layers of the exocuticle with a specific crystallographic orientation suggests a mechanical function related to specific external loading patterns, most probably related to wear- and impact resistance.

4. Experimental

Sample Preparation: Samples were dissected from the exoskeleton of a male, nonmolting American lobster (*Homarus americanus*) acquired from a local seafood supplier. The stage of the molt cycle was determined according to Waddy et al. [46] as intermolt (C4), indicated by the presence of the membranous layer on the inner surface of the cuticle, the uniformly hard carapace with firm and light colored lower margins, the clear white ventral abdomen and the absence of epidermal retraction at the pleopod tips. Samples were extracted from different positions in the dorsal part of the carapace which contains a higher amount of calcite than other exoskeleton components. For the pole figure measurements, the specimens were cut with a diamond saw to roughly 1×10 mm, with the third dimension amounting to the cuticle thickness which is also roughly 1 mm. This geometry avoids variations in sample volume irradiated by the X-ray beam. The specimens were washed shortly in distilled water and rinsed in 100% methanol. For X-ray microbeam measurements, a cross-sectional slice of lobster cuticle with a thickness of about 70 μm was prepared using a low speed diamond saw without water cooling to avoid dissolution of ACC. All samples were stored at a temperature of $-30\,^{\circ}$C until they were mounted for the respective diffraction experiments which lasted typically 60–120 minutes. A second sample from a different animal with a thickness of about 100 μm was prepared in the same way and used for the *in-situ* heating experiments.

X-Ray Diffraction: Crystallographic texture was determined by calculating pole figures from wide-angle X-ray diffraction measurements in transmission mode [30]. The measurements were performed employing X-rays of a wavelength $\lambda = 0.8$ Å with a beam size of 1 mm at the SCD-beamline of the ANKA synchrotron radiation facility (Karlsruhe, Germany). The samples were mounted on copper tips and were placed on a fixed chi (54.7°) goniometer, equipped with a 62 mm × 62 mm CCD area detector (Smart Apex, Bruker AXS). The sample was rotated in 60 steps around its longest axis perpendicular to the primary beam from 0° to 180°, and 2D diffraction patterns were acquired for each step. Exposure time for each frame ranged from 60 to 180 seconds. After correction for background, sample geometry and intensity normalization, pole figures were calculated from the diffraction data.

Scanning X-ray diffraction experiments were carried out at the μ-Spot beamline at the synchrotron radiation facility BESSY II in Berlin [47] using a monochromatic X-ray beam from a multilayer with a wavelength of $\lambda = 0.827$ Å. The x-ray beam was focused in both, horizontal and vertical directions by a toroidal mirror and finally defined by a pinhole of 10 μm diameter located close to the sample. The cuticle cross-sections were mounted on glass tips and placed on the goniometer stage of the instrument. Specimen visualization was possible with an on-axis long distance optical microscope. 2D

diffraction images were taken with a MarMosaic-225 detector (Mar, Evanston, USA) as a function of sample position coordinates. Several linear scans and a few area scans covering the whole cuticle cross section (epicuticle, exocuticle and endocuticle) were performed with a step size of 10 μm. Furthermore, an in situ heating experiment combined with microbeam scanning X-ray diffraction was performed by gluing the cross sectional slice of the second sample to the tip of a thermocouple and heating it with a mirror lamp [34]. Temperature was ramped from room temperature to 450 °C in steps of 25 °C, and an X-ray diffraction line scan across the whole cuticle was performed for each temperature.

[1] A. Neville, *The Biology of the Arthropod Cuticle*, Springer, Berlin **1975**.

[2] S. Weiner, P. M. Dove, in *Reviews in Mineralogy and Geochemistry, Biomineralization*, Vol. 54 (Eds: P. M. Dove, J. J. De Yoreo, S. Weiner), Mineralogical Society of America and The Geochemical Society, Washington D. C. **2003**, p. 1.

[3] F. Boßelmann, P. Romano, H. Fabritius, D. Raabe, M. Epple, *Thermochim. Acta* **2007**, *463*, 65.

[4] F. Neues, A. Ziegler, M. Epple, *CrystEngComm* **2007**, *9*, 1245.

[5] F. C. Meldrum, *Int. Mater. Rev.* **2003**, *48*, 187.

[6] L. Addadi, S. Raz, S. Weiner, *Adv. Mater.* **2003**, *15*, 959.

[7] J. Aizenberg, G. Lambert, L. Addadi, S. Weiner, *Adv. Mater.* **1996**, *8*, 222.

[8] J. Aizenberg, G. Lambert, S. Weiner, L. Addadi, *J. Am. Chem. Soc.* **2002**, *124*, 32.

[9] A. Becker, U. Bismayer, M. Epple, H. Fabritius, B. Hasse, J. M. Shi, A. Ziegler, *Dalton Trans.* **2003**, 551.

[10] A. Becker, A. Ziegler, M. Epple, *Dalton Trans.* **2005**, 1814.

[11] S. Raz, O. Testeniere, A. Hecker, S. Weiner, G. Luquet, *Biol. Bull.* **2002**, *203*, 269.

[12] S. Weiner, L. Addadi, *J. Mater. Chem.* **1997**, *7*, 689.

[13] S. Weiner, L. Hood, *Science* **1975**, *190*, 987.

[14] S. Weiner, W. Traub, *Philos. Trans. R. Soc. London Ser. B* **1984**, *304*, 425.

[15] M. M. Giraud-Guille, *Tissue Cell* **1984**, *16*, 75.

[16] M. M. Giraud-Guille, C. Quintana, *Biol. Cell* **1982**, *44*, 57.

[17] M. M. Giraud-Guille, E. Belamie, G. Mosser, *C. R. Palevol* **2004**, *3*, 503.

[18] R. Dillaman, S. Hequembourg, M. Gay, *J. Morphol.* **2005**, *263*, 356.

[19] R. Roer, R. Dillaman, *Am. Zool.* **1984**, *24*, 893.

[20] G. L. Becker, C. H. Chen, J. W. Greenawa, A. L. Lehninge, *J. Cell Biol.* **1974**, *61*, 316.

[21] A. Neville, *Biology of Fibrous Composites*, Cambridge University Press, Cambridge **1993**.

[22] J. Blackwell, M. A. Weih, *J. Mol. Biol.* **1980**, *137*, 49.

[23] D. Raabe, P. Romano, C. Sachs, A. Al-Sawalmih, H. G. Brokmeier, S. B. Yi, G. Servos, H. G. Hartwig, *J. Cryst. Growth* **2005**, *283*, 1.

[24] M. M. Giraud-Guille, *Int. Rev. Cytol.* **1996**, *166*, 59.

[25] M. M. Giraud-Guille, *Curr. Opin. Solid State Mater. Sci.* **1998**, *3*, 221.

[26] Y. Bouligand, *Tissue Cell* **1972**, *4*, 189.

[27] D. Raabe, A. Al-Sawalmih, S. B. Yi, H. Fabritius, *Acta Biomater.* **2007**, *3*, 882.

[28] V. T. C. Chang, R. J. P. Williams, A. Makishima, N. S. Belshawl, R. K. O'Nions, *Biochem. Biophys. Res. Commun.* **2004**, *323*, 79.

FULL PAPER

[29] S. Raz, S. Weiner, L. Addadi, *Adv. Mater.* **2000**, *12*, 38.

[30] H.-J. Bunge, *Texture Analysis in Materials Science*, Cuvillier, Göttingen **1993**.

[31] R. Minke, J. Blackwell, *J. Mol. Biol.* **1978**, *120*, 167.

[32] S. Mann, *Biomineralization*, Oxford University Press, Oxford **2001**.

[33] D. Raabe, P. Romano, C. Sachs, H. Fabritius, A. Al-Sawalmih, S. Yi, G. Servos, H. G. Hartwig, *Mater. Sci. Eng. A* **2006**, *421*, 143.

[34] G. A. Zickler, W. Wagermaier, S. S. Funari, M. Burghammer, O. Paris, *J. Anal. Appl. Pyrol.* **2007**, *80*, 134.

[35] E. DiMasi, M. Sarikaya, *J. Mater. Res.* **2004**, *19*, 1471.

[36] D. Chateigner, C. Hedegaard, H. R. Wenke, *J. Struct. Geol.* **2000**, *22*, 1723.

[37] A. R. Terepka, *Exp. Cell Res.* **1963**, *30*, 171.

[38] A. H. Parsons, *Poult. Sci.* **1982**, *61*, 2013.

[39] T. Hegdahl, F. Gustavsen, J. Silness, *Zool. Scr.* **1977**, *6*, 101.

[40] T. Hegdahl, J. Silness, F. Gustavsen, *Zool. Scr.* **1977**, *6*, 89.

[41] M. M. Giraud-Guille, *Cell Tissue Res.* **1984**, *236*, 413.

[42] A. B. Rodriguez-Navarro, C. CabraldeMelo, N. Batista, N. Morimoto, P. Alvarez-Lloret, M. Ortega-Huertas, V. M. Fuenzalida, J. I. Arias, J. P. Wiff, J. L. Arias, *J. Struct. Biol.* **2006**, *156*, 355.

[43] Y. Levi-Kalisman, S. Raz, S. Weiner, L. Addadi, I. Sagi, *Adv. Funct. Mater.* **2002**, *12*, 43.

[44] S. A. Wainwright, W. D. Biggs, J. D. Currey, J. M. Gosline, *Mechanical Design in Organisms*, Princeton University Press, Princeton, NJ **1982**.

[45] C. Sachs, H. Fabritius, D. Raabe, *J. Mater. Res.* **2006**, *21*, 1987.

[46] S. L. Waddy, D. E. Aiken, D. P. V. De Kleijn, in *Biology of the Lobster Homarus americanus* (Ed: J.R. Factor), Academic, New York **1995**, p. 217.

[47] O. Paris, C. H. Li, S. Siegel, G. Weseloh, F. Emmerling, H. Riesemeier, A. Erko, P. Fratzl, *J. Appl. Crystallogr.* **2007**, *40*, S466.